Research Article

Fat mass and obesity-associated protein downregulation trigger the activation of the sirtuin 1/forkhead box O1 signaling pathway, drive glycolysis, and promote the progression of renal cell carcinoma

Zheng Zhang, MM[1], Jifeng Zhang, MM[2], Renzhong Zhang, MM[3]*

Departments of [1]Hemodialysis, [2]Oncology, [3]Nephrology, Zibo Central Hospital, Zibo, China.

*Corresponding author:

Renzhong Zhang,
Department of Nephrology,
Zibo Central Hospital, Zibo,
China.

zhangrenzhong1977@163.com

ABSTRACT

Objective: This study aims to investigate the role of fat mass and obesity-associated protein (FTO) in renal clear cell carcinoma (RCC), particularly its regulatory effects on glycolysis, cell proliferation, and sirtuin 1/forkhead box O1 (SIRT1/FOXO1) signaling pathway.

Material and Methods: The messenger RNA and protein expression levels of FTO in human proximal tubular epithelial cells (human kidney 2 [HK-2]) and the RCC cell line A498 were determined by quantitative reverse transcription polymerase chain reaction and Western blot. FTO expression was downregulated by FTO short hairpin RNA and overexpressed using plasmids. Glycolysis levels were assessed by measuring glucose uptake, lactate secretion, extracellular acidification rate, and adenosine triphosphate/adenosine diphosphate (ATP/ADP) ratio. The effects of FTO on cell proliferation and cell cycle were evaluated through colony formation assays, 5-ethynyl-2′-deoxyuridine (EdU) staining, and flow cytometry. The SIRT1/FOXO1 signaling pathway was analyzed through Western blot, and FOXO1 pathway inhibitor (AS1842856) was used to further explore the role of SIRT1/FOXO1 in the FTO-mediated regulation of RCC.

Results: FTO was downregulated in A498 cells compared with that in HK-2 cells. FTO downregulation markedly increased glucose uptake, lactate secretion, and the ATP/ADP ratio in A498 cells, and its overexpression inhibited these processes. FTO downregulation also promoted RCC cell proliferation, as evidenced by an increase in colony formation and the number of EdU-positive cells. Meanwhile, FTO overexpression suppressed the proliferation of these cells. Flow cytometry analysis revealed that FTO downregulation notably increased the proportion of cells in the S phase, and its overexpression increased the proportion of cells in the G0/G1 phase. Further analysis indicated that FTO downregulation activated the SIRT1/FOXO1 signaling pathway, and its overexpression inhibited this pathway. Treatment with the FOXO1 inhibitor AS1842856 significantly reversed the pro-glycolysis and pro-proliferation effects of FTO downregulation, supporting the role of the SIRT1/FOXO1 pathway in FTO-mediated regulation.

Conclusion: FTO downregulation promotes glycolysis and proliferation in RCC cells by activating the SIRT1/FOXO1 signaling pathway. Targeting the FTO and SIRT1/FOXO1 pathway may provide potential therapeutic strategies for the treatment of RCC.

Keywords: Fat mass and obesity-associated protein, Glycolysis, Proliferation, Renal cell carcinoma

INTRODUCTION

Renal cell carcinoma (RCC) is a type of cancer that originates in the kidneys, and it is responsible for the majority of kidney cancer cases, representing 85–90% of all kidney tumors.[1,2] RCC typically lacks evident clinical symptoms in its early stages and is poorly sensitive to radiotherapy and chemotherapy. As a result, many patients are already at an advanced stage by the time of diagnosis, having missed the optimal window for surgical treatment.[3] Although emerging therapies such as targeted treatments and immunotherapy have shown some efficacy in treating RCC, the prognosis for advanced RCC remains poor due to the high risk of drug resistance and tumor recurrence.[4] Elucidating the biological processes underlying RCC development and identifying new therapeutic targets are crucial to improve the prognosis of patients with RCC patients.

The reprogramming of tumor metabolism, especially the aberrant activation of the glycolytic pathway (Warburg effect), is one of the key biological features in RCC progression.[5,6] Tumor cells preferentially use glycolysis for energy production, even when oxygen levels are adequate, instead of utilizing the more energy-efficient oxidative phosphorylation pathway.[7] This metabolic shift provides the energy required for tumor cell growth and proliferation and generates a large number of metabolic intermediates that contribute to the formation of the tumor microenvironment.[8,9] Therefore, a deep understanding of the regulatory mechanisms associated with glycolysis may provide new insights for metabolic interventions in RCC.

Fat mass and obesity-associated protein (FTO) is an RNA demethylase that regulates RNA metabolism processes, including RNA stability, splicing, and translation, by removing m6A modifications.[10] The role of FTO in various malignancies has gained widespread attention, with its function differing across different tumors.[11,12] For example, FTO contributes to the progression of acute myeloid leukemia[13] and exhibits tumor-suppressive effects in pancreatic cancer and thyroid cancer.[14,15] To date, systematic research on the expression profiles and cellular functions of FTO in RCC is still lacking. Whether FTO is involved in the metabolic shift of RCC cells, particularly in glycolysis, requires further investigation.

The sirtuin 1/forkhead box O1 (SIRT1/FOXO1) signaling pathway is a highly regarded pathway in cell metabolism regulation.[16] SIRT1 is a nicotinamide adenine dinucleotide (NAD+)-dependent deacetylase that regulates various downstream targets, including FOXO1, through deacetylation.[17,18] FOXO1 can control the expression of glycolysis-related genes (such as glucose transporter 1 [GLUT1] and lactate dehydrogenase A [LDHA]) and play either inhibitory or promotive roles in the development of various tumors.[19] SIRT1 activates FOXO1 through deacetylation, thereby regulating cell metabolism and proliferation.[20] Whether FTO regulates glycolysis and proliferation in RCC cells through the SIRT1/FOXO1 signaling pathway remains to be clarified.

Based on the above background, this study aims to explore the expression pattern of FTO in RCC and systematically analyze its role in glycolysis and proliferation in RCC cells. The potential regulatory mechanisms by which FTO modulates RCC metabolism and proliferation through the SIRT1/FOXO1 signaling pathway are also investigated. We hypothesize that FTO downregulation activates the SIRT1/FOXO1 signaling pathway, thereby promoting glycolysis and proliferation in RCC cells. By revealing the role of FTO in RCC metabolic reprogramming, this study aims to provide new molecular targets and potential therapeutic strategies for the treatment of RCC.

MATERIAL AND METHODS

Cell culture

Human RCC cell line A498 (iCell-h010) and human renal tubular epithelial cell line human kidney 2 (HK-2) (iCell-h096) were obtained from Cellverse (Shanghai, China). The cells were cultured in Dulbecco's Modified Eagle Medium (DMEM) (iCell-0001, Cellverse, Shanghai, China) containing 10% fetal bovine serum (iCell-0500) and 1% penicillin/streptomycin (iCell-15140-122, Cellverse, Shanghai, China). The culture was maintained in an incubator at 37°C with 5% carbon dioxide (CO_2). The cells used in this study were authenticated by short tandem repeat identification (STR) analysis, and the mycoplasma test yielded negative results.

Cell transfection and treatment

A498 cells in good condition were seeded evenly in a six-well plate. FTO overexpression plasmid and short hairpin RNA (shRNA) (FTO) were obtained from Sangon Biotech (Shanghai, China) and diluted in serum-free medium. The diluted DNA was gently mixed with Lipofectamine 3000 transfection reagent (L3000001, Thermo, Waltham, Massachusetts, USA) and incubated at 25°C for 10 min to form the DNA–transfection reagent complex. The prepared transfection reagent–DNA complex was added to the cells (500 μL), which were incubated in a 37°C, 5% CO_2 incubator (MCO-170AIC, Panasonic, Osaka, Japan) for 4 h while avoiding any disturbance. After 4 h, replace with complete medium and continue incubation for 24 h.

The non-transfected and short hairpin RNA-fat mass and obesity-associated protein (sh-FTO)-transfected A498 cells were treated with AS1842856 (AS) at a concentration of 10 μM.

Quantitative reverse transcription polymerase chain reaction

RNA was extracted from the cells using an RNA extraction reagent (DP420, Tiangen, Beijing, China), and its purity and concentration were measured. The RNA was reverse-transcribed into complementary DNA (cDNA) using a cDNA synthesis kit (KR108, Tiangen, Beijing, China). A reaction mixture containing SYBR Green Master Mix, forward and reverse primers, and the cDNA template was prepared and subjected to qPCR. Cycle threshold (CT) values were analyzed using qPCR software, and relative expression levels were calculated using the $2^{-\Delta\Delta CT}$ method. β-actin was used as the internal control for normalization. The primer sequences involved in this study are detailed in Table 1.

Western blot

The cells were lysed using a special lysis buffer (R0010, Solarbio, Beijing, China) to collect the protein. Protein concentration was measured using a Bicinchoninic Acid Assay Kit (PC0020, Solarbio, Beijing, China). According to the protein size, the appropriate concentration of sodium dodecyl sulfate-polyacrylamide gel electrophoresis gel was selected (G2037-50T, Servicebio, Wuhan, China). Load the samples and run electrophoresis to separate the proteins by molecular weight. The proteins were transferred from the gel to a polyvinylidene fluoride membrane (G6015, Servicebio, Wuhan, China), which was then blocked with 5% bovine serum albumin solution (GC305010, Servicebio, Wuhan, China) at room temperature for 1 h. Incubated the membrane with primary antibodies at 4°C overnight: FTO (1:1000, GB111359, Servicebio, Wuhan, China), SIRT1 (1:1000, GB11512, Servicebio, Wuhan, China), FOXO1 (1:1000, GB11495, Servicebio, Wuhan, China), and β-actin (1:1000, GB15003, Servicebio, Wuhan, China). The membrane was washed three times with TBST buffer for 5 min each and then incubated with HRP-labeled secondary antibody (1:1000, GB23303, Servicebio, Wuhan, China)

Table 1: Primes sequences.

Primes name	Primes sequences
hum-FTO-F	GGATGAGCCAGCTTCACTGT
hum-FTO-R	AGAAGGGTGCGATTTCTGGG
hum-GLUT1-F	TGAGCATCGTGGCCATCTTT
hum-GLUT1-R	AGGCATGGAACCATTCAGGG
hum-LDHA-F	CATGGCCTGTGCCATCAGTA
hum-LDHA-R	AGATATCCACTTTGCCAGAGACA
hum-β-actin-F	GTGGATATTGTTGCCATCAATGACC
hum-β-actin-R	GCCCCAGCCTTCTTCATGGTGGT

hum: Human, GLUT1: Glucose transporter 1, LDHA: Lactate dehydrogenase A, A: Adenine, C: Cytosine, G: Guanine, T: Thymine

solution. An Enhanced Chemiluminescence substrate (G2020, Servicebio, Wuhan, China) was used to incubate the membrane, and protein bands were detected using an imaging system (Gel Doc EZ, Bio-Rad Laboratories, Hercules, California, USA). Band intensity was analyzed using ImageJ software (version 1.5f, National Institutes of Health, Bethesda, Maryland, USA).

Enzyme-linked immunosorbent assay (ELISA)

Glucose measurement

The cells were cultivated in a glucose-free medium for 80 min. The culture medium was harvested, followed by centrifugation to eliminate any cell debris. A glucose detection kit (60408ES60, Yeasen Biotechnology, Shanghai, China) was used in accordance with the manufacturer's instructions. The sample, enzyme reaction reagent, and chromogenic agent were mixed and incubated at 37°C for 30 min to ensure complete color development. The absorbance at 450 nm was recorded using a microplate reader (ELx808, Agilent, Santa Clara, California, USA), and the glucose content was calculated.

Lactate measurement

The cells were placed under culture conditions, and the culture supernatant was collected. A lactate detection kit was used (D799851, Sangon Biotech, Shanghai, China). The sample was mixed with the detection buffer, lactate dehydrogenase, and coenzyme NAD+ and incubated at 37°C for 30 min. The absorbance at 490 nm was recorded using a microplate reader (ELx808, Agilent, Santa Clara, California, USA), and the lactate concentration was calculated.

ATP/ADP ratio measurement

ATP measurement

ATP content assay kits (MAK473, Merck, Rahway, New Jersey, USA) were purchased. The cells were collected and lysed to extract total proteins and other components, obtaining an ATP solution. The ATP solution was mixed with ATP enzymes (glucose kinase), substrates (NADH), and other relevant enzymes, catalyzing the reaction to generate a measurable colored compound. The absorbance at 340 nm was recorded using a microplate reader, and the ATP concentration was calculated by comparing it with the standard curve.

ADP measurement

ADP content assay kits (MAK518, Merck, Rahway, New Jersey, USA) were purchased. The cells were lysed with lysis buffer to obtain a clear extract and then mixed with luciferase substrate, ATPase, and appropriate buffer. Measure the

luminescence intensity of the samples using a luminometer. Compare the luminescence intensity of the samples with the standard curve to calculate the ADP concentration.

ATP/ADP ratio = ATP concentration/ADP concentration

Extracellular acidification rate (ECAR) analysis

First, the cells were seeded into a culture plate containing a culture medium without carbon sources to avoid interference and then incubated at 37°C. The pH changes in the extracellular medium were measured using the Seahorse analyzer (XFe96, Agilent Technologies, Santa Clara, California, USA). Different metabolic stimulators (glucose, oligomycin, and 2-DG) were injected to influence the glycolysis reaction, and the ECAR was calculated.

Colony formation assay

Approximately 1000 cells/well were seeded and allowed to adhere to a culture plate and then incubated in a 37°C, 5% CO_2 environment for 14 days. If drug treatment was required, the drug was added during the incubation period. After the culture medium was removed, the cells were fixed with a fixative, followed by staining with crystal violet solution (G1014, Servicebio, Wuhan, China) for 10 min. An inverted microscope (IX83, Olympus, Tokyo, Japan) was used to observe and count colonies larger than 50 μm.

EdU staining

First, the cells were incubated at an appropriate density. After 10 μM EdU solution (GDP1023, Servicebio, Wuhan, China) was added, incubation was continued for 1 h to incorporate EdU into the newly synthesized DNA. Then, fix the cells. Next, perform the click reaction by combining Alexa Fluor 488 with EdU and incubating for 30 min. For nucleus visualization, the cells were stained with DAPI (G1047, Servicebio, Wuhan, China) for 5 min and observed under a fluorescence microscope (LSM 980, Carl Zeiss, Oberkochen, Baden-Württemberg, Germany).

Flow cytometry

First, the cells were collected using trypsin and centrifuged to remove the supernatant. The cells were resuspended, and their concentration was adjusted to 1×10^6 cells/mL. The cells were fixed with 70% ice-cold ethanol, mixed thoroughly, and stored at −20°C for 1 h. After fixation, the cells were washed with PBS to remove the ethanol.

The cells were stained with DNA dye (propidium iodide, PI) (G1021, Servicebio, Wuhan, China). A working solution with a PI concentration of 50 μg/mL was prepared. RNase A (G3405, Servicebio, Wuhan, China) (50 μg/mL) was added during staining to remove RNA interference. After staining, the cells were incubated at 25°C in the dark for 30 min and washed with PBS to remove excess dye.

The cells were analyzed using flow cytometry (BD LSRFortessa X-20, BD Biosciences, Parsippany, New Jersey, USA) by setting the detection channels appropriate for the dye's wavelength. The cell populations were differentiated using forward scatter and side scatter. PI-stained cells in the red fluorescence channel were detected. Flow cytometry software (BD FACSDiva 9.x, BD Biosciences, Parsippany, New Jersey, USA) was used to analyze the data and plot the cell cycle distribution. According to their DNA content, the cells were divided into G0/G1 phase, S phase, and G2/M phase.

CCK-8 assay

The cells from different treatment groups were treated into a 96-well plate at approximately 1×10^5 cells per well and cultured for 48 h. Each well was added with 10 μL of CCK-8 reagent (G4103, Servicebio, Wuhan, China) and gently shaken. The plate was incubated for 2 h, during which the CCK-8 reagent reacted with the cells to generate an orange-yellow dye. The optical density value of each well was measured at 450 nm using a microplate reader ((ELx808, Agilent, Santa Clara, California, USA).
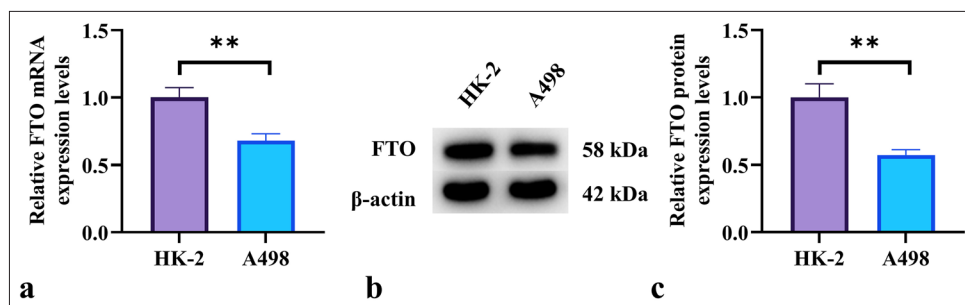
Figure 1: Downregulation of FTO expression in RCC. (a) qRT-PCR analysis of FTO mRNA levels in RCC cell line (A498) and renal tubular epithelial cell line (HK-2). (b and c) Western blot analysis of FTO protein levels in A498 and HK-2 cells. *n* = 6. **P<0.01. FTO: Fat mass and obesity-associated protein, qRT-PCR: Quantitative reverse transcription polymerase chain reaction, RCC: Renal clear cell carcinoma, mRNA: Messenger RNA, HK-2: Human kidney 2.

Statistical analysis

Statistical analysis was conducted using GraphPad Prism software (version 9.0, GraphPad Software Inc., San Diego, California, USA). Intergroup comparisons were performed using *t*-tests and one-way Analysis of Variance, followed by Tukey's *post hoc* test. Data were presented as mean ± standard deviation. A $P < 0.05$ was considered statistically significant.

RESULTS

FTO expression is downregulated in RCC

To assess the expression pattern of FTO in RCC cells, we measured the messenger RNA (mRNA) and protein levels of

FTO in the HK-2 cells and the A498 cells. Figures 1a-c show that the mRNA and protein expression levels of FTO were significantly downregulated in the A498 cells compared with those in the HK-2 cells ($P < 0.01$).

FTO knockdown promotes glycolysis in RCC cells

This study further investigated the effects of FTO knockdown and overexpression on glycolysis in RCC cells. We used FTO ShRNA and FTO overexpression plasmids for loss-of-function and gain-of-function studies. Figure 2a shows the transfection efficiency of FTO knockdown and overexpression in the A498 cells. Among the Sh-FTO constructs, Sh-FTO-(3) exhibited the highest knockdown
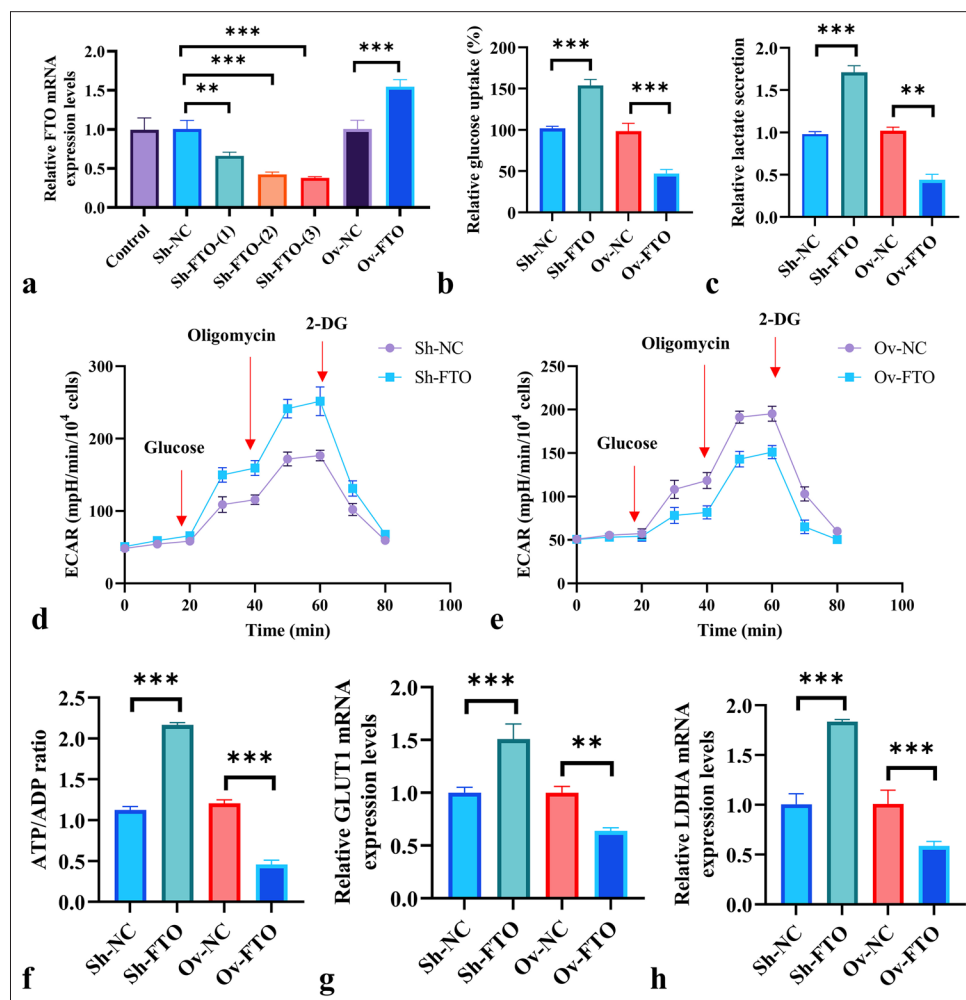
Figure 2: FTO knockdown promotes glycolysis in RCC cells. (a) Verification of FTO knockdown and overexpression efficiency using qRT-PCR after ShRNA and overexpression plasmid transfection. (b-c) Measurement of glucose uptake and lactate secretion levels. (d-e) Measurement of ECAR levels in A498 cells after transfection. (f) ATP/ADP ratio measurement. (g and h) Effect of FTO knockdown and overexpression on GLUT1 and LDHA mRNA levels. $n = 6$. **$P < 0.01$, ***$P < 0.001$. FTO: Fat mass and obesity-associated protein, RCC: Renal clear cell carcinoma, GLUT1: Glucose transporter 1, LDHA: Lactate dehydrogenase A, ATP/ADP: Adenosine triphosphate/adenosine diphosphate, mRNA: Messenger RNA, ECAR: Extracellular acidification rate, qRT-PCR: Quantitative reverse transcription polymerase chain reaction, ShRNA: Short hairpin RNA.

efficiency ($P < 0.001$) and, therefore, was selected for the knockdown experiments and subsequently referred to as Sh-FTO. In addition, Ov-FTO successfully overexpressed the FTO gene in the A498 cells ($P < 0.001$). Figures 2b and c show that FTO knockdown significantly increased glucose uptake and lactate secretion in the A498 cells, and its overexpression markedly decreased glucose uptake and lactate secretion ($P < 0.01$, $P < 0.001$). Figures 2d and e demonstrate that the baseline glycolysis, maximum glycolytic capacity, and glycolytic reserve in the A498 cells were all enhanced following Sh-FTO transfection compared with those in the Sh-NC group. Conversely, these parameters were suppressed in the RCC cells after Ov-FTO transfection. Furthermore, FTO knockdown significantly increased the ATP/ADP ratio compared with that in the Sh-NC group, and its overexpression notably inhibited the ATP/ADP ratio ($P < 0.001$) [Figure 2f]. Figures 2g and h indicate that FTO knockdown significantly increased the mRNA expression of GLUT1 and LDHA, and its overexpression significantly reduced the mRNA expression of GLUT1 and LDHA ($P < 0.01$, $P < 0.001$).

FTO knockdown promotes the proliferation of RCC cells

Colony formation assay results showed that FTO knockdown significantly increased the number of colonies formed by the A498 cells ($P < 0.001$), and its overexpression showed the opposite ($P < 0.001$) [Figure 3a and b]. EdU fluorescence staining results demonstrated that, compared with that in the negative control group, the number of EdU-positive cells significantly increased after FTO knockdown but significantly decreased after FTO overexpression ($P < 0.001$) [Figure 3c and d].

Flow cytometry results [Figure 4a-d] indicated that FTO knockdown significantly reduced the number of cells in the G0/G1 phase and increased that in the S phase ($P < 0.001$). By contrast, FTO overexpression led to a significant increase in the number of cells in the G0/G1 phase and a decrease in
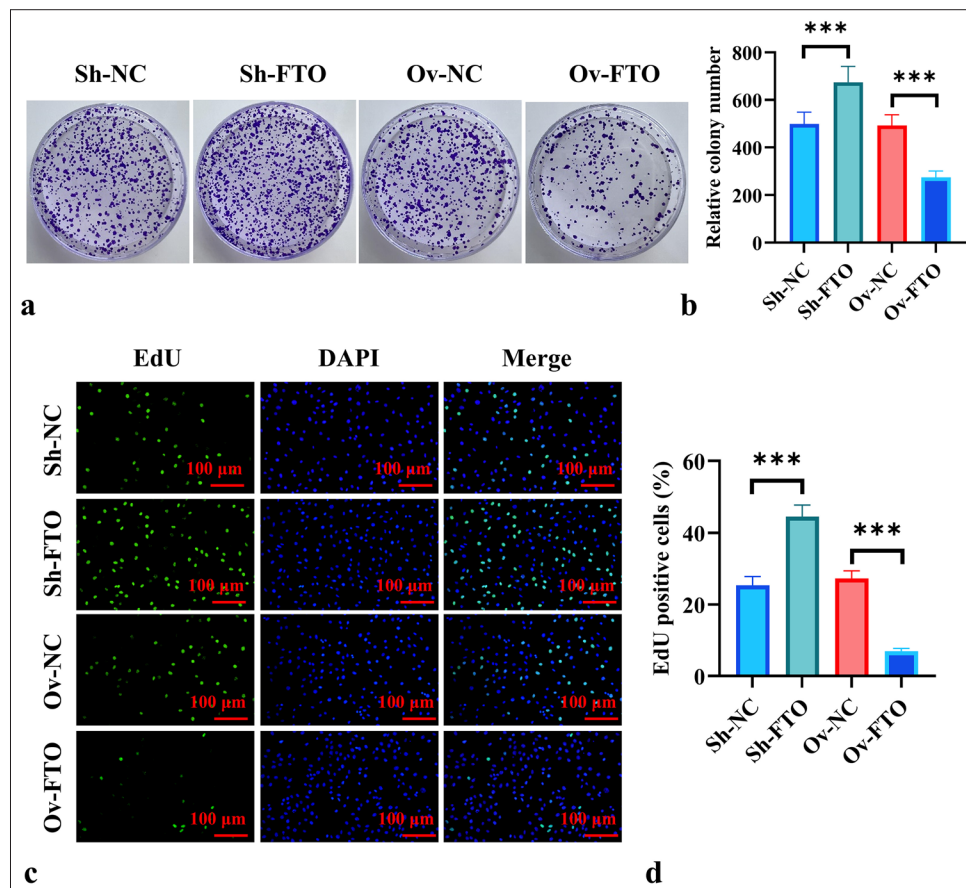
Figure 3: FTO knockdown promotes the proliferation of RCC cells. (a and b) Effects of FTO knockdown and overexpression on cell colony formation. (c and d) Effects of FTO knockdown and overexpression on the number of EdU-positive cells in A498 cells. Scale bar: 100 μm. Magnification: ×200. $n = 6$. ***$P < 0.001$. FTO: Fat mass and obesity-associated protein, RCC: Renal clear cell carcinoma, EdU: 5-ethynyl-2′-deoxyuridine.
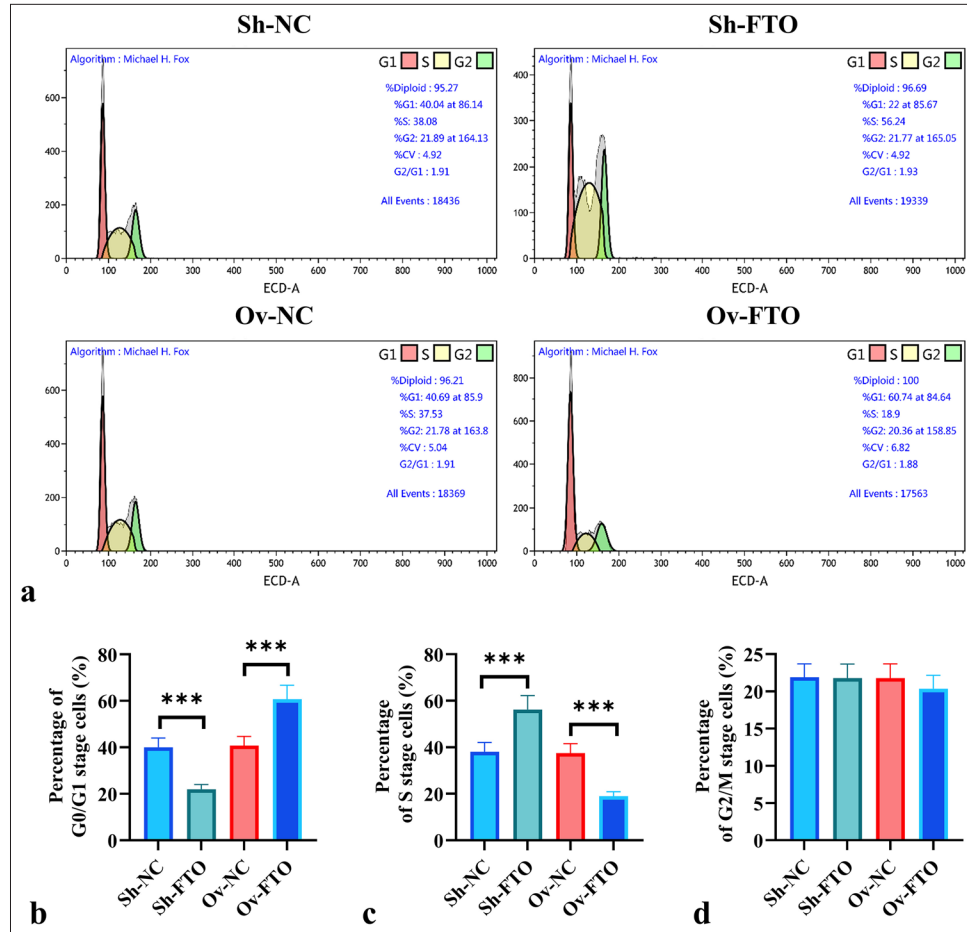
Figure 4: Effect of FTO on the cell cycle of RCC cells. (a-d) Flow cytometry analysis of the effects of FTO knockdown and overexpression on the cell proliferation cycle in A498 cells. $n = 6$. ***$P < 0.001$. FTO: Fat mass and obesity-associated protein, RCC: Renal clear cell carcinoma.

the S phase ($P < 0.001$). No significant effect on the G2/M phase was observed after FTO knockdown or overexpression in the A498 cells.

FTO knockdown activates the SIRT1/FOXO1 signaling pathway

We conducted the following studies to investigate the potential molecular mechanisms of FTO in RCC. Western blot analysis was used to assess the effects of FTO knockdown and overexpression on the protein levels of SIRT1 and FOXO1 in A498 cells. Figures 5a-c show that FTO knockdown significantly increased the protein expression of SIRT1 and FOXO1 ($P < 0.001$), and its overexpression had the opposite effect ($P < 0.001$). To further confirm that FTO knockdown activates the SIRT1/FOXO1 signaling pathway, we added the FOXO1 signaling pathway inhibitor AS1842856 (AS) for subsequent experiments. Figures 5d-f show that the protein expression of SIRT1 and FOXO1 was significantly higher in the Sh-FTO+AS group than in the AS group ($P < 0.001$). By

contrast, the protein expression of SIRT1 and FOXO1 was significantly lower in the Sh-FTO+AS group than in the Sh-FTO group ($P < 0.001$). These results suggested that AS addition significantly reversed the activation of the SIRT1/FOXO1 signaling pathway induced by Sh-FTO.

FTO regulates the glycolysis and proliferation of RCC cells through the SIRT1/FOXO1 signaling pathway

Figures 6a-c show that compared with the AS group, the Sh-FTO+AS group exhibited significantly increased glucose uptake, lactate production, and ATP/ADP ratio ($P < 0.01$). Compared with the Sh-FTO group, the Sh-FTO+AS group showed a significant decrease in glucose uptake, lactate production, and ATP/ADP ratio ($P < 0.001$). AS addition significantly inhibited the mRNA expression of GLUT1 and LDHA. Figures 6d and e show that the mRNA expression of GLUT1 and LDHA in the Sh-FTO+AS group was significantly higher than that in the AS group ($P < 0.001$) and significantly lower than that in the Sh-FTO group ($P < 0.001$).
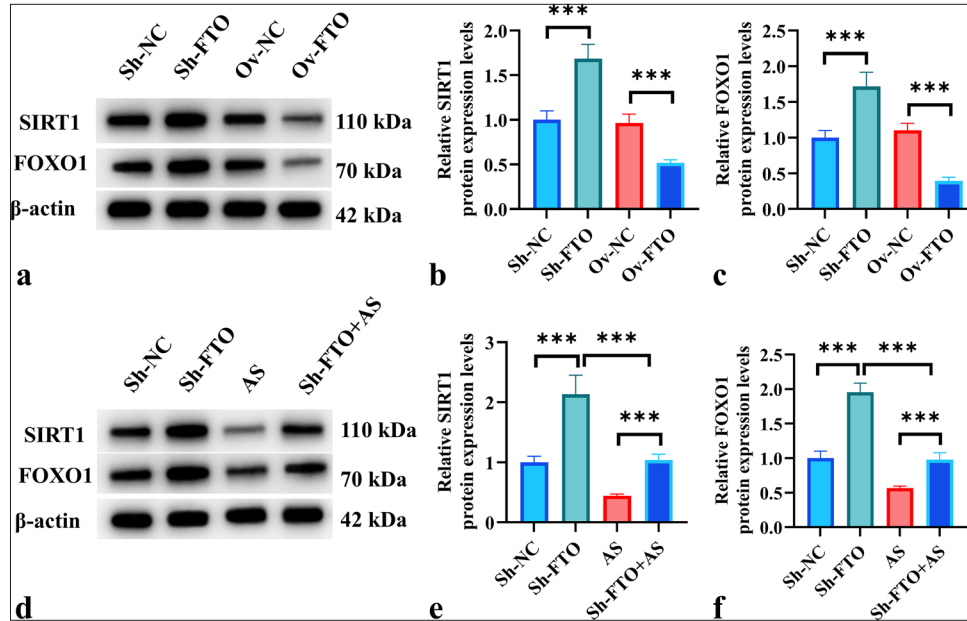
Figure 5: FTO knockdown activates the SIRT1/FOXO1 signaling pathway. (a-c) Effects of FTO knockdown and overexpression on the protein expression of SIRT1 and FOXO1. (d-f) Effects of the FOXO1 signaling pathway inhibitor AS1842856 and/or Sh-FTO on the protein expression of SIRT1 and FOXO1. $n = 6$. ***$P < 0.001$. FTO: Fat mass and obesity-associated protein, SIRT1/FOXO1: Sirtuin 1/Forkhead box O1.

CCK-8 assay results showed that cell viability in the Sh-FTO+AS group was significantly higher than in the AS group but significantly lower than that in the Sh-FTO group ($P <0.001$) [Figure 6f].

Figures 7a-d show that compared with the Sh-FTO group, the Sh-FTO+AS group had a significantly increased percentage of cells in the G0/G1 phase and a significantly reduced percentage of cells in the S phase ($P < 0.001$). Compared with the AS group, the Sh-FTO+AS group had a significantly reduced percentage of cells in the G0/G1 phase and a significantly increased percentage of cells in the S phase ($P < 0.001$). Sh-FTO or/and AS treatment did not affect the cells in the G2/M phase.

DISCUSSION

This study demonstrates that FTO is significantly downregulated in RCC cells compared with that in normal proximal renal tubular epithelial cells. This finding is consistent with previous research showing FTO downregulation in various cancer types, including thyroid and colon cancer.[14,21] Our study further reveals that FTO knockdown promotes glycolysis and proliferation in RCC cells, and its overexpression has the opposite effect. This result suggests that FTO may act as a tumor suppressor in RCC, primarily by regulating metabolic reprogramming and cell proliferation.

The metabolic reprogramming observed in our study aligns with increasing evidence that cancer cells tend to shift their energy metabolism toward aerobic glycolysis, known as the Warburg effect.[22] In A498 cells, FTO knockdown led to an increase in glucose uptake, lactate production, and glycolytic capacity, accompanied by an elevated ATP/ADP ratio. These results are consistent with other studies showing that changes in RNA methylation can regulate metabolic pathways in colorectal cancer.[23] In addition, the upregulation of glycolysis-related genes GLUT1 and LDHA induced by FTO knockdown provides new insight into the mechanism by which FTO inhibits glycolysis in RCC cells. Similar findings were verified in papillary thyroid carcinoma, where FTO loss promotes glycolysis and tumor progression.[24]

A major highlight of this study is the first discovery that the SIRT1/FOXO1 signaling pathway is a key downstream target of FTO in RCC cells. Our results indicate that FTO knockdown activates the SIRT1/FOXO1 signaling pathway, as evidenced by the increase in SIRT1 and FOXO1 protein levels. Previous studies emphasized the tumor-promotion roles of SIRT1 and FOXO1 in cholangiocarcinoma.[25] The activation of the SIRT1/FOXO1 pathway following FTO knockdown may be the cause of enhanced glycolysis and increased cell proliferation, as the SIRT1/FOXO1 signaling pathway has been shown to be involved in glucose metabolism and cell cycle regulation.[26]
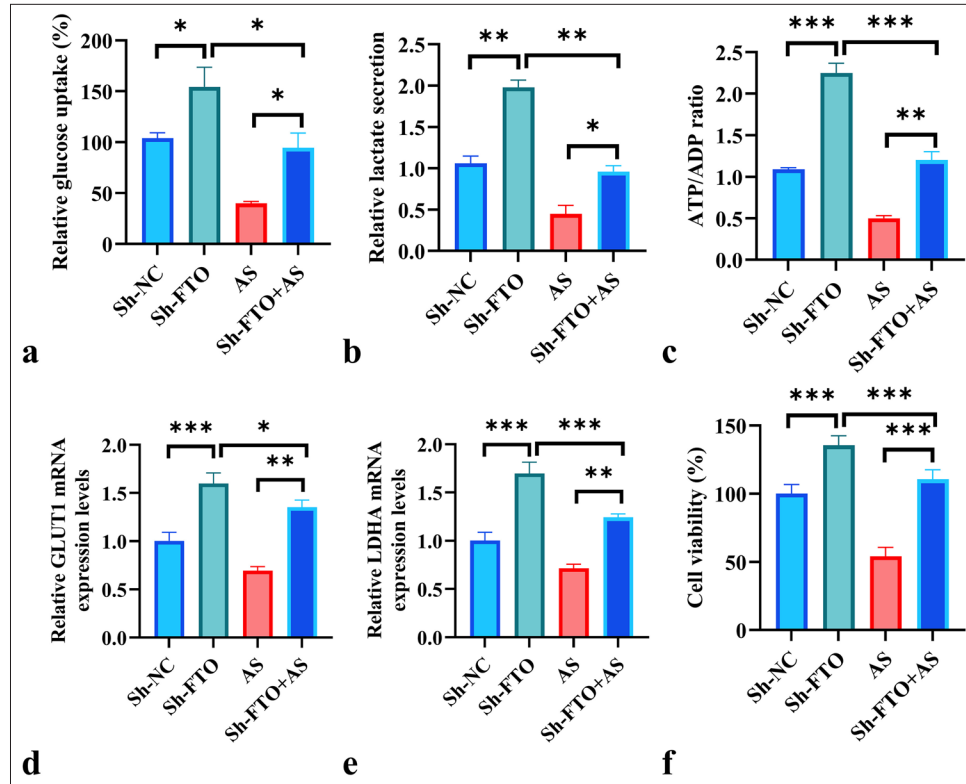
Figure 6: FTO regulates the glycolysis and proliferation of RCC cells through the SIRT1/FOXO1 signaling pathway. (a-c) Effects of AS and/or Sh-FTO on glucose uptake, lactate secretion levels, and ATP/ADP ratio. (d and e) Effects of AS and/or Sh-FTO on GLUT1 and LDHA mRNA levels. (f) Effects of AS and/or Sh-FTO on A498 cell viability. $n = 6$. *$P < 0.05$, **$P < 0.01$, ***$P < 0.001$. FTO: Fat mass and obesity-associated protein, RCC: Renal clear cell carcinoma, SIRT1/FOXO1: Sirtuin 1/Forkhead box O1, GLUT1: Glucose transporter 1, LDHA: Lactate dehydrogenase A, ATP/ADP: Adenosine triphosphate/adenosine diphosphate, mRNA: Messenger RNA.

Adding the FOXO1 inhibitor, AS1842856 reverses the effects of FTO knockdown on the SIRT1/FOXO1 pathway, glycolysis, and proliferation, further confirming the role of this signaling axis in the FTO-mediated regulation of RCC cell behavior. This finding is consistent with previous studies showing that FOXO1 suppression can diminish its regulatory effects on metabolism and the cell cycle.[27] Moreover, our data suggest that the metabolic and proliferative changes triggered by FTO knockdown largely depend on the activation of the SIRT1/FOXO1 signaling pathway, indicating that this pathway may serve as a potential therapeutic target in RCC.

In terms of cell proliferation, our results show that FTO knockdown significantly promotes colony formation and cell cycle progression, as evidenced by an increase in the proportion of S-phase cells and a decrease in G0/G1-phase cells. This finding is consistent with the role of FOXO1 as a key regulator of the cell cycle, where its inhibition has been linked to enhanced cell proliferation in various types of cancer.[28] Our findings also align with other studies reporting that reduced FTO expression is associated with increased tumor growth and aggressiveness.[29]

This study has several strengths. First, using FTO knockdown and overexpression models, it systematically elucidates the functional role of FTO in RCC. This bidirectional regulation strategy provides robust data supporting a deep understanding of FTO's function. Second, this research is the first to reveal the molecular mechanism by which FTO regulates glycolysis and proliferation in RCC cells through the SIRT1/FOXO1 signaling pathway. This discovery offers new insights into metabolic reprogramming in RCC and provides a basis for future potential targeted therapies. Finally, we employed various cell function assays, such as glycolysis analysis, cell proliferation analysis, and cell cycle analysis, to validate FTO's biological effects from multiple perspectives, enhancing the scientific rigor and credibility of the results.

Despite uncovering the potential role of FTO in RCC, this work still has some limitations. First, our study was primarily conducted *in vitro*, lacking *in vivo* validation. Therefore, the relevance of FTO's regulation of RCC through the SIRT1/FOXO1 pathway in animal models and its clinical applicability still require further investigation. Second,
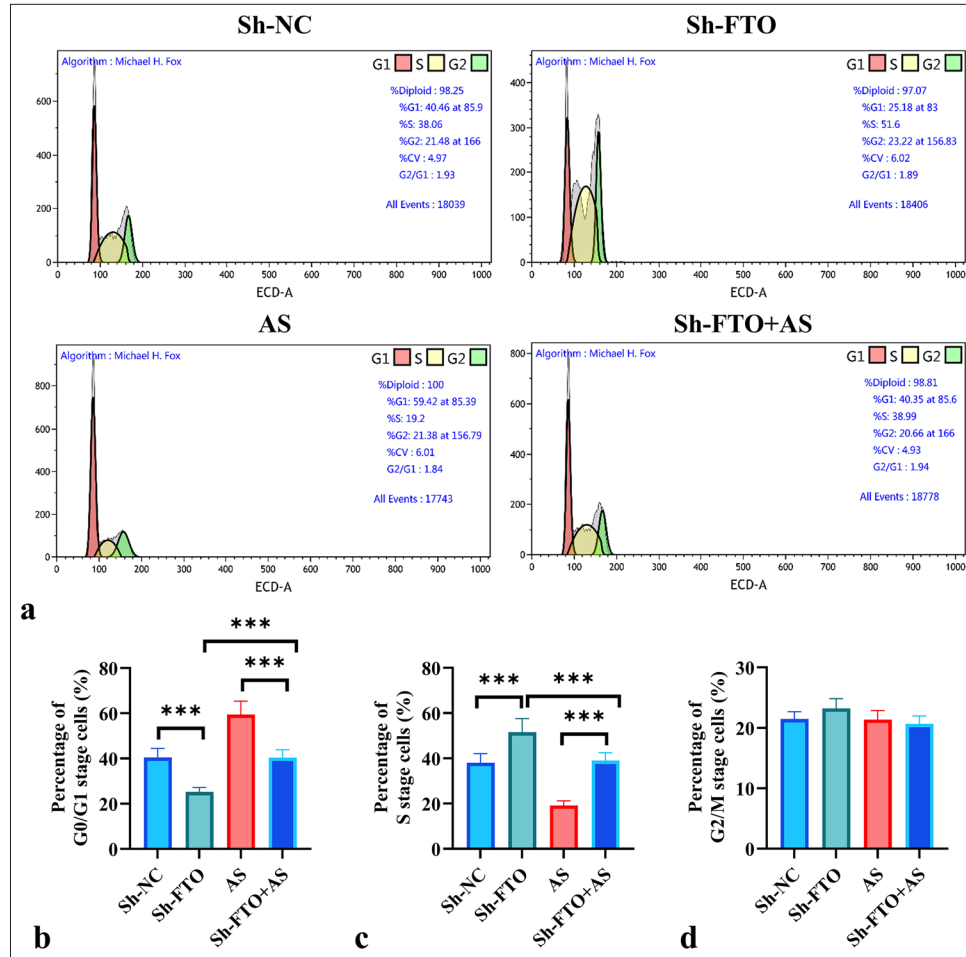
Figure 7: FTO regulates the cell proliferation cycle of RCC cells through the SIRT1/FOXO1 signaling pathway. (a-d) Effects of AS1842856 (AS) and/or Sh-FTO on A498 cell proliferation cycle. *n* = 6. ***P < 0.001. FTO: Fat mass and obesity-associated protein, RCC: Renal clear cell carcinoma, SIRT1/FOXO1: Sirtuin 1/Forkhead box O1.

this study focused solely on the SIRT1/FOXO1 signaling pathway; FTO may influence tumor progression through other downstream pathways. Future research should explore FTO's interaction with other potential signaling networks. In addition, this study only used the A498 cell line; future work should extend to other RCC cell lines or primary cells to strengthen the generalizability of the results.

SUMMARY

This study provides new insights into the tumor-suppressive role of FTO in RCC, showing that its downregulation promotes glycolysis and cell proliferation by activating the SIRT1/FOXO1 signaling pathway. Our findings deepen the understanding of FTO's function in RCC and suggest that the SIRT1/FOXO1 signaling pathway could be a potential target for RCC therapy. Future research should further explore the molecular mechanisms by which FTO regulates glycolysis

and cell proliferation and validate its clinical relevance in RCC through *in vivo* experiments.

AVAILABILITY OF DATA AND MATERIALS

The data that support the findings of this study are available from the corresponding author upon reasonable request.

ABBREVIATIONS

A: Adenine
ATP/ADP: Adenosine triphosphate/adenosine diphosphate
C: Cytosine
ECAR: Extracellular acidification rate
EdU: 5-ethynyl-2′-deoxyuridine
FTO: Fat mass and obesity-associated protein
G: Guanine
GLUT1: Glucose transporter 1

HK-2: Human kidney 2
hum: Human
LDHA: Lactate dehydrogenase A
mRNA: Messenger RNA
qRT-PCR: Quantitative reverse transcription polymerase chain reaction
RCC: Renal clear cell carcinoma
ShRNA: Short hairpin RNA
SIRT1/FOXO1: Sirtuin 1/Forkhead box O1
T: Thymine

AUTHOR CONTRIBUTIONS

ZZ: Conceived and designed the study; ZZ, JFZ, and RZZ: Responsible for data acquisition; ZZ: Analyzed and interpreted the data; JFZ and RZZ: Responsible for experiments; ZZ: Drafted the first version of the manuscript; ZZ, JFZ, and RZZ: Critically revised the manuscript. All authors meet the ICMJE authorship criteria.

ETHICS APPROVAL AND CONSENT TO PARTICIPATE

Ethical approval and consent to participate is not required as this study does not involve animal or human experiments.

ACKNOWLEDGMENT

FUNDING

CONFLICT OF INTEREST

The authors declare no conflict of interest.

EDITORIAL/PEER REVIEW

To ensure the integrity and highest quality of CytoJournal publications, the review process of this manuscript was conducted under a **double-blind model** (authors are blinded for reviewers and vice versa) through an automatic online system.

REFERENCES

1. Bahadoram S, Davoodi M, Hassanzadeh S, Bahadoram M, Barahman M, Mafakher L. Renal cell carcinoma: An overview of the epidemiology, diagnosis, and treatment. G Ital Nefrol 2022;39:2022-vol3.
2. Chen YW, Wang L, Panian J, Dhanji S, Derweesh I, Rose B, *et al.* Treatment landscape of renal cell carcinoma. Curr Treat Options Oncol 2023;24:1889-916.
3. Gebrael G, Sahu KK, Agarwal N, Maughan BL. Update on combined immunotherapy for the treatment of advanced renal cell carcinoma. Hum Vaccin Immunother 2023;19:2193528.
4. Choueiri TK, Powles T, Burotto M, Escudier B, Bourlon MT, Zurawski B, *et al.* Nivolumab plus cabozantinib versus sunitinib for advanced renal-cell carcinoma. N Engl J Med 2021;384:829-41.
5. He Y, Wang X, Lu W, Zhang D, Huang L, Luo Y, *et al.* PGK1 contributes to tumorigenesis and sorafenib resistance of renal clear cell carcinoma via activating CXCR4/ERK signaling pathway and accelerating glycolysis. Cell Death Dis 2022;13:118.
6. Wu J, Miao C, Wang Y, Wang S, Wang Z, Liu Y, *et al.* SPTBN1 abrogates renal clear cell carcinoma progression via glycolysis reprogramming in a GPT2-dependent manner. J Transl Med 2022;20:603.
7. Wu L, Jin Y, Zhao X, Tang K, Zhao Y, Tong L, *et al.* Tumor aerobic glycolysis confers immune evasion through modulating sensitivity to t cell-mediated bystander killing via TNF-α. Cell Metab 2023;35:1580-96.e89.
8. Wang L, Liu Y, Dai Y, Tang X, Yin T, Wang C, *et al.* Single-cell RNA-seq analysis reveals BHLHE40-driven pro-tumour neutrophils with hyperactivated glycolysis in pancreatic tumour microenvironment. Gut 2023;72:958-71.
9. Kooshan Z, Cárdenas-Piedra L, Clements J, Batra J. Glycolysis, the sweet appetite of the tumor microenvironment. Cancer Lett 2024;600:217156.
10. Liu Y, Liang G, Xu H, Dong W, Dong Z, Qiu Z, *et al.* Tumors exploit FTO-mediated regulation of glycolytic metabolism to evade immune surveillance. Cell Metab 2021;33:1221-33.e11.
11. Chen X, Wang Y, Wang JN, Zhang YC, Zhang YR, Sun RX, *et al.* Lactylation-driven FTO targets CDK2 to aggravate microvascular anomalies in diabetic retinopathy. EMBO Mol Med 2024;16:294-318.
12. Chen A, Zhang VX, Zhang Q, Sze KM, Tian L, Huang H, *et al.* Targeting the oncogenic m6A demethylase FTO suppresses tumourigenesis and potentiates immune response in hepatocellular carcinoma. Gut 2024;74:90-102.
13. Zhou W, Li S, Wang H, Zhou J, Li S, Chen G, *et al.* A novel AML1-ETO/FTO positive feedback loop promotes leukemogenesis and Ara-C resistance via stabilizing IGFBP2 in t(8;21) acute myeloid leukemia. Exp Hematol Oncol 2024;13:9.
14. Ji FH, Fu XH, Li GQ, He Q, Qiu XG. FTO prevents thyroid cancer progression by SLC7A11 m6A methylation in a ferroptosis-dependent manner. Front Endocrinol (Lausanne) 2022;13:857765.
15. Lin K, Zhou E, Shi T, Zhang S, Zhang J, Zheng Z, *et al.* M6a eraser FTO impairs gemcitabine resistance in pancreatic cancer through influencing NEDD4 mRNA stability by regulating the PTEN/PI3K/AKT pathway. J Exp Clin Cancer Res 2023;42:217.
16. Liang C, Xing H, Wang C, Xu X, Hao Y, Qiu B. Resveratrol improves the progression of osteoarthritis by regulating the SIRT1-FoxO1 pathway-mediated cholesterol metabolism. Mediators Inflamm 2023;2023:2936236.
17. Zhu M, Wei C, Wang H, Han S, Cai L, Li X, *et al.* SIRT1 mediated gastric cancer progression under glucose deprivation through the FoxO1-Rab7-autophagy axis. Front Oncol 2023;13:1175151.

18. Zhang S, Lu Y, Shi W, Ren Y, Xiao K, Chen W, *et al.* SIRT1/FOXO1 axis-mediated hippocampal angiogenesis is involved in the antidepressant effect of Chaihu shugan san. Drug Des Devel Ther 2022;16:2783-801.

19. Sun D, Chen S, Li S, Wang N, Zhang S, Xu L, *et al.* Enhancement of glycolysis-dependent DNA repair regulated by FOXO1 knockdown via PFKFB3 attenuates hyperglycemia-induced endothelial oxidative stress injury. Redox Biol 2023;59:102589.

20. Luchetti F, Nasoni MG, Burattini S, Mohammadi A, Pagliarini M, Canonico B, *et al.* Melatonin attenuates ischemic-like cell injury by promoting autophagosome maturation via the sirt1/FoxO1/Rab7 axis in hippocampal HT22 cells and in organotypic cultures. Cells 2022;11:3701.

21. Qiao Y, Su M, Zhao H, Liu H, Wang C, Dai X, *et al.* Targeting FTO induces colorectal cancer ferroptotic cell death by decreasing SLC7A11/GPX4 expression. J Exp Clin Cancer Res 2024;43:108.

22. Alberghina L. The warburg effect explained: Integration of enhanced glycolysis with heterogeneous mitochondria to promote cancer cell proliferation. Int J Mol Sci 2023;24:15787.

23. Zhuang J, Lin C, Ye J. m^{6}A RNA methylation regulators contribute to malignant progression in rectal cancer. J Cell Physiol 2020;235:6300-6.

24. Huang J, Sun W, Wang Z, Lv C, Zhang T, Zhang D, *et al.* FTO suppresses glycolysis and growth of papillary thyroid cancer via decreasing stability of APOE mRNA in an N6-methyladenosine-dependent manner. J Exp Clin Cancer Res 2022;41:42.

25. Xin C, Wang X, Li X, Chen Y, Wang X, Ning J, *et al.* Silencing SIRT1 reduces 5-fluorouracil resistance of cholangiocarcinoma cells by inhibiting the FOXO1/Rab7 autophagy pathway. Nan Fang Yi Ke Da Xue Xue Bao 2023;43:454-9.

26. Ren BC, Zhang YF, Liu SS, Cheng XJ, Yang X, Cui XG, *et al.* Curcumin alleviates oxidative stress and inhibits apoptosis in diabetic cardiomyopathy via Sirt1-Foxo1 and PI3K-Akt signalling pathways. J Cell Mol Med 2020;24:12355-67.

27. Zhang L, Liang B, Xu H, Gong Y, Hu W, Jin Z, *et al.* Cinobufagin induces FOXO1-regulated apoptosis, proliferation, migration, and invasion by inhibiting G9a in non-small-cell lung cancer A549 cells. J Ethnopharmacol 2022;291:115095.

28. Cui Y, Wu X, Jin J, Man W, Li J, Li X, *et al.* CircHERC1 promotes non-small cell lung cancer cell progression by sequestering FOXO1 in the cytoplasm and regulating the miR-142-3p-HMGB1 axis. Mol Cancer 2023;22:179.

29. Fan H, Zhao S, Ai R, Niu X, Zhang J, Liu L. FOXO1-induced miR-502-3p suppresses colorectal cancer cell growth through targeting CDK6. J Oncol 2023;2023:2541391.